THE FLOW STRUCTURE NEAR THE WINDWARD SIDE OF V-SHAPED WINGS WITH AN ATTACHED SHOCK WAVE ON THE LEADING EDGES

M. A. Zubin and N. A. Ostapenko

UDC 533.6.011.72

The results of a numerical calculation of a symmetric flow of supersonic gas with the Mach number M = 3 past the windward side of V-shaped wings with an opening angle $\gamma = 40^\circ$ and apex angles $\beta = 30, 45$, and 90° are given. The possibility of the ascent of one or two Ferri points from the break point of the transverse contour of the wing is discovered and explained. It is shown that conical flow near wings of finite length need not exist in flow regimes corresponding to angles of attack α at which a Ferri point ascends, while at angles of attack smaller and larger than a certain interval, conical flow will exist. The investigation is conducted by means of a numerical method of stabilization with an artificial viscosity. The longitudinal coordinate, relative to which the steady system of equations is hyperbolic, played the part of the time variable, usual for methods of stabilization. The numerical method constructed using the scheme of [1] is described in [2] and was successfully applied to the calculation of different regimes of supersonic flow past conical wings with supersonic leading edges [2-6]. In the present investigation the calculation algorithm of [2] is modified and makes it possible to realize motion with respect to the parameter α, this being particularly important for the stabilization of the solution in the calculation of flow regimes for which regions with a total velocity Mach number close to unity arise in the flow.

Figure 1 gives the structures of the characteristic lines near V-shaped wings with the above parameters of the geometry for the number M = 3 in the plane normal to the break line of the wing for the angle of attack $\alpha \to 0$. The continuous lines are the wakes of the shock waves, and the broken lines, those of the Mach cones. As can be seen, the wings selected ensure a wide variety of flow regimes and wave configurations as the angle of attack is increased.

We note that the V-shaped wings with the apex angles $\beta = 45$ and 90° (Figs. 1b, 1c) do not have standard flow regimes for M = 3 with the plane shock wave on the leading edges, whereas a standard flow regime occurs on the wing with the angle $\beta = 30^\circ$ (Fig. 1a) for the angle of attack $\alpha = 33.8^\circ$ with a shock wave belonging to the strong family in the planes normal to the leading edges.

Without dwelling on the description of the flow regimes of V-shaped wings as the angle of attack is increased, this being the topic of a special discussion with a general nature, we note only that near the wing with the angle $\beta = 30^\circ$ for as little as $\alpha = 5^\circ$ a Mach interaction of the shock reflected from the point 1 (Fig. 1a) with the wall will be observed, while for $\alpha = 8.9^\circ$ it will belong to the strong family of the plane normal to the reflection line and impinge normally on the wall of the wing. Thus, for $\alpha = 8.9^\circ$, we will speak of the standard flow regime of an inner V-shaped wing with a strong shock wave in the plane normal to the leading edge, for which the point 1 (Fig. 1a) is the wake of the leading edge, while the wall of the initial wing is the plane of flow symmetry. The uniform flow behind the plane shock wave attached to the leading edge of the initial wing is the unperturbed flow for the inner wing. For $\alpha > 8.9^\circ$ a Mach configuration of the shock waves near the wing with the angle $\beta = 30^\circ$ is observed.

For the wing with the angle $\beta = 45^\circ$ the standard flow regime near the inner wing with the leading edge (1) (Fig. 1b) is realized for the angle of attack $\alpha = 24.8^\circ$, but

Moscow. Translated from Izvestiya Akademii Nauk SSSR, Mekhanika Zhidkosti i Gaza, No. 1, pp. 122-131, January-February, 1986. Original article submitted April 21, 1985.

0015-4628/86/2101-0104$12.50

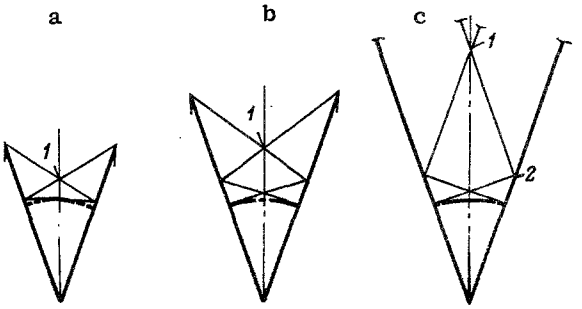

Fig. 1

near the inner wing (1) (Fig. 1c, $\beta = 90^\circ$) it does not occur at all in the range of angles of attack preceding the angle of attack at which regions with a total velocity equal to the critical velocity appear in the perturbed flow. In view of the last fact, the numerical calculation of the flow past the V-shaped wing with the angle $\beta = 90^\circ$ was carried out only for the inner wing with the leading edge (1) (Fig. 1c) located in a uniform supersonic flow along the wall of the initial wing.

The continuous curves in Figs. 2a and 2b give the distributions of the pressure coefficient C_p over the wall of the wing (the left curves 1) and in the plane of flow symmetry (the right curves 1), obtained in the numerical calculation of the flow past the wing with the angle $\beta = 30^\circ$ for the angles of attack $\alpha = 9^\circ$ (Fig. 2a) and $\alpha = 32^\circ$ (Fig. 2b) as a dependence of the coordinate $\eta = \tan \varphi$, where φ is the angle measured from the edge of the wing along its wall or in the plane of flow symmetry.

Since the shock fronts in the continuous calculation schemes are smeared, the exact position of the shock wave was determined using the position of the maximum pressure gradient and all the necessary parameters behind it were calculated. The pressure levels thus obtained are smoothly linked by the broken curves 2 with the basic pressure level obtained in the numerical calculation in the neighborhood of the shock waves. The point K (see the structure of the shock waves in the transverse plane near the wing, Figs. 2a and 2b) denotes the position of the leading edge of the wing and the pressure level behind the plane shock attached to it, while the points K_1 and K_2, respectively, denote the locations of the internal shock wave on the wall of the wing and the bridge-shaped shock of the Mach configuration of shock waves in the plane of flow symmetry, and also the calculated values of the pressure behind them.

The fairly large pressure drops in the narrow zone behind the shock wave (Fig. 2a) are not worked through by the difference scheme because of the small number of grid points in the region indicated. In the same place, where the extent of these zones is greater (Fig. 2b), the corresponding pressure distribution is partially stabilized in the numerical solution. The chain lines 3 show the pressure levels on an equivalent wedge, either in a uniform flow along the wall of the wing, or in an unperturbed flow, and set angles of attack which the indicated flows make with the relative to them at the chord of the V-shaped wing.

The examples shown in Fig. 2 of the calculation of the flow past the V-shaped wing with the apex angle $\beta = 30^\circ$ correspond to the flow regimes when flow with a shock wave detached from the leading edges occurs near the inner wing in the flow behind the plane shock wave attached to the leading edge [7] ($\sigma > 8.9^\circ$), while, because of this, flow with a Mach configuration of the shock waves occurs near the main wing.

An interesting result discovered in the calculations is the relative position of the inner and bridge-shaped shocks in the Mach interaction of the shock waves near the V-shaped wings relative to the shocks on the equivalent wedges. Figure 3 gives the corresponding dependences for the wing with the apex angle $\beta = 30^\circ$. Curve 1 is the position θ of the internal shock wave on the wall of the wing, curve 2 is the position of the shock on the equivalent wedge relative to the direction of the uniform flow behind the plane shock wave attached to the leading edge, and curves 3 and 4 are the positions of the closing shock wave and the shock on the equivalent wedge in the symmetry plane of the flow. Curves 1 and 3 are bounded on the right by the value of the angle of attack $\alpha = 33.5^\circ$, up to which the calculation was made. The points 5

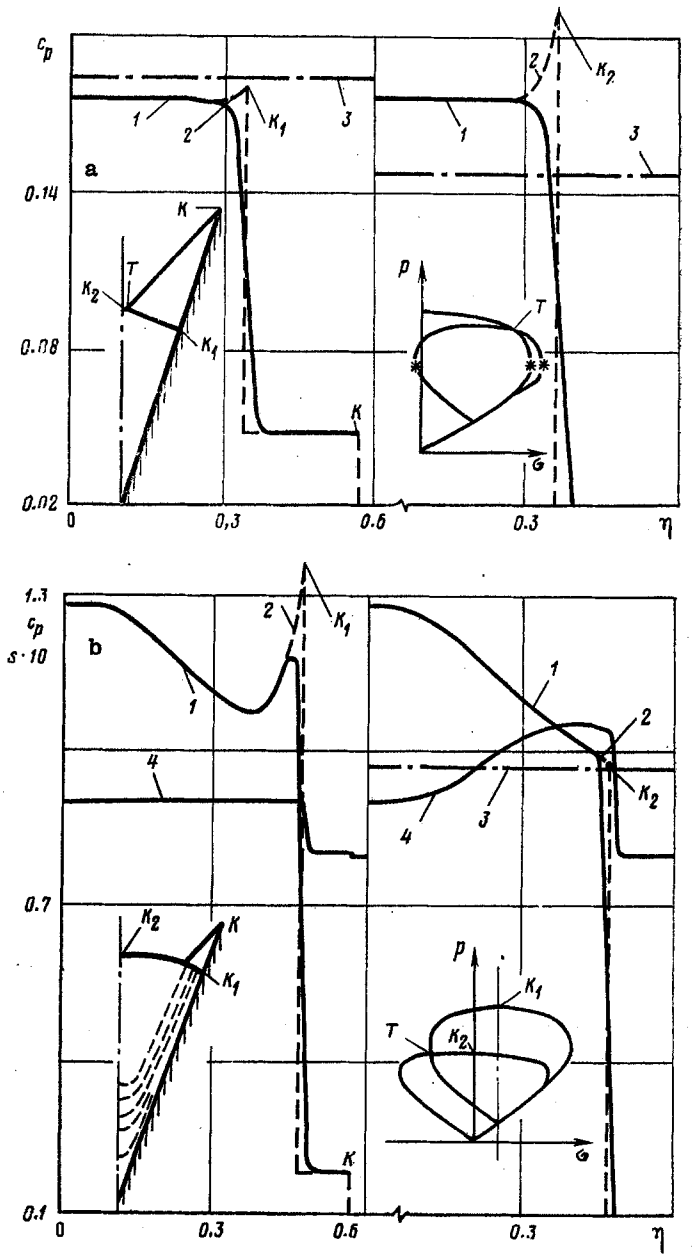

Fig. 2

and 6 denote the regimes in which, respectively, the critical velocity behind the shock on the equivalent wedge is reached, and the standard flow regime is realized, toward which the position of the bridge-shaped shock tends on the axis of flow symmetry as $\alpha \to 33.8^\circ$. The intersection of the curves 1 and 2 corresponds to the standard regime of flow past the inner wing for $\alpha = 8.9^\circ$. The jump θ on curves 3 and 4 is also associated with it, since for $\alpha = 8.9^\circ$ there occurs an abrupt transition from the conditions in the uniform flow behind the shock reflected from the plane of symmetry to the conditions in the unperturbed flow in the changeover of the structure of the flow past the initial wing from normal to Mach shock wave interaction.

The internal shock wave in the Mach configuration of shock waves lags behind the shock wave on the equivalent wedge both near the initial wing (Fig. 3, curve 1, $\alpha > 8.9^\circ$) and near the inner V-shaped wing (curve 3, $\alpha < 8.9^\circ$) whereas the bridge-shaped shock in the symmetry plane of the corresponding wing (curve 1, $\alpha < 8.9^\circ$, curve 3, $\alpha > 8.9^\circ$) outstrips the shock on the equivalent wedge. Hence it follows that in the symmetry plane of the flow in the presence of a Mach configuration of shock waves the streamline behind the bridge-shaped shock will be directed from the edge of the wing, whereas behind the internal shock on the wall, it will be directed toward the edge of the wing.

The rule discovered is reflected both in the pressure levels behind the inner and bridge-shaped shocks and behind the shock waves on the equivalent wedges (Figs. 2a, 2b).

The analysis of the results of the calculation of the flow past the V-shaped wing with the apex angle $\beta = 30^\circ$ for angles of attack $\alpha < 8.9^\circ$, when a Mach configuration of shock waves is realized near the inner wing, showed that in the interior flow region a mean pressure level develops that is below the pressure level on the equivalent wedges. At the same time, the streamlines of three-dimensional flow running along the wall of the wing and passing the bridge-shaped shock near the inner wing are directed from the edge of the wing, whereas the streamlines in the neighborhood of the plane of symmetry, passing the inner shock, are directed toward the edge of the wing. The former, subjected to a negative pressure gradient, acquire a negative curvature and the latter, subjected to a positive pressure gradient, acquire a positive curvature, if the abscissa of the coordinate system in each of the planes is made to coincide with the edge of the wing, while the ordinates are directed to the side of the oncoming flow, and asymptotically downstream, they acquire the same direction as the direction of the edge of the V-shaped wing. Thus, for $\alpha < 8.9^\circ$, the streamlines of the conical flow on the sphere enter the Ferri point which is the same as the break point of the transverse contour of the wing.

For the angles of attack $8.9^\circ < \alpha \leq 14^\circ$ (Fig. 2a) the mean pressure level in the interior flow region is lower than both pressure levels behind the shock waves, but higher than the pressure on the equivalent wedge in the unperturbed flow. Behind the internal shock wave K_1 the streamlines running along the wall of the wing are directed toward the edge of the wing, while the streamlines in the neighborhood of the plane of symmetry K_2 are directed away from the edge. It would seem that the former must have a positive curvature and the pressure must increase from the point K_1 toward the edge of the wing. However, the presence of a minimum in the pressure distribution (Fig. 2a) indicates that the streamlines in a certain neighborhood of the point K_1, like the streamlines passing the shock K_2, have a negative curvature, i.e., they increase the slope in the direction of the edge of the wing, but then, changing the direction of the convexity under the influence of the positive pressure gradient, asymptotically acquire the same direction as the edge of the wing.

The pressure drops observed behind the jumps K_1 and K_2, but not the equalization, are associated with the lower pressure in the interior flow region in the neighborhood of the triple point T (Fig. 2a) of the Mach shock wave interaction, whose parameters are determined by the point of intersection T of the shock polars given there; p is the pressure and σ is the angle of deviation of the flow. Therefore, even for $8.9^\circ < \alpha \leq 14^\circ$, the Ferri point is at the break point of the transverse contour of the wing. This is also confirmed by the distributions of the entropy function s (not given). The entropy behind the wave K_1 along the wall of the wing is constant. It is also constant behind the wave K_2 on the axis of flow symmetry, decreasing slightly in the small neighborhood of the edge of the wing to the entropy level on the wall of the wing, this being associated with the spreading of the Ferri singularity in the numerical solution.

The nature of the flow in the perturbed region changes qualitatively for angles of attack $\alpha > 14^\circ$ (Fig. 2b).

A distinguishing feature of these flow regimes is the lower pressure level behind the bridge-shaped shock K_2 than the mean pressure level in the interior flow region, although its intensity exceeds the shock wave intensity on the equivalent wedge in the unperturbed flow. This indicates that the streamlines passing the shock K_2 and directed from the edge of the wing have a positive curvature and continue to deviate from the edge, while the Ferri point rises from the wing surface and is no longer at the break point of its cross section.

This qualitatively new type of flow in the shock layer is traced well using the distribution of the entropy function s in the plane of flow symmetry (the right-hand curve 4 in Fig. 2b). Two regions with constant entropies are observed. One is in the neighborhood of the edge of the wing with the same entropy level as on the wall of the wing (the left-hand curve 4 in Fig. 2b) and the second is behind the shock wave K_2. The transition section between the two entropy levels indicated in the neighborhood of the center of the elliptical flow region corresponds to the spreading of the Ferri singular point in the numerical solution.

On the flow scheme near the wing in the transverse plane (Fig. 2b) to the right of the line of symmetry, by means of the analysis of the flow field parameters obtained in the numerical calculation, we have plotted isentrope streamlines for which the value of the entropy function varies from 0.091 near the wall to 0.099 in the neighborhood of the triple point T. The isentrope picture confirms the presence of a streamline structure in the conical flow with the Ferri point that has ascended.

We note that the interpretation of the results of the calculation given in [8] on the basis of the distribution of the total velocity components in the plane normal to the chord of the V-shaped wing, and the streamline scheme given in the interior flow region are invalid.

We turn to the question of the reasons leading to the ascending of the Ferri point.

The interaction of the shock polars in the planes normal to the conical rays passing through the triple points T of the Mach shock wave configuration obtained in the numerical solution is shown qualitatively in Fig. 2b for $\alpha > 14^\circ$. Analysis showed that the pressures behind the internal shock K_1 and behind the bow shock K_2 on the axis of symmetry are practically the same as the pressure maxima on the internal and main polars, respectively. This is associated with the small variation of the Mach number of the flow normal to both the generators of the conical internal shock in the region behind the shock wave attached to the leading edge and to the generators of the bridge-shaped shock in the unperturbed region, this occurring for V-shaped wings with large opening angles for large angles of attack. Therefore, in similar cases, we can draw sufficiently accurate conclusions about the pressure distribution behind the bridge-shaped and internal shocks from the calculation of the shock polar interaction at the triple points of the Mach shock wave configuration (Fig. 2b, segments TK_2 and TK_1 of the shock polars, respectively).

The presence of such regimes of flow past V-shaped wings indicates that in the conical flow on a sphere there is an analogy with plane supersonic gas flows [9], in which the total pressure losses in the normal shock exceed the total pressure losses in the oblique—normal shock system. In the calculations, the ascent of the Ferri point is observed when the Mach numbers of the unperturbed flow normal to the conical ray passing through the triple point T of the Mach shock wave configuration are $M_n > 1.5$. For precisely such Mach numbers, in accordance with the data of [9], the coefficient of restitution of total pressure in the oblique—normal shock system exceeds the coefficient of restitution of total pressure in the normal shock. In the examples of the calculation given, $M_n = 1.46$ for $\alpha = 9^\circ$ (Fig. 2a) and $M_n = 2.5$ for $\alpha = 32^\circ$ (Fig. 2b).

Thus, in the flow on the sphere in the neighborhood of the wall of the wing, gas particles with a higher total pressure than the particles passing the bridge-shaped shock are present. They also determine the nature of the flow in the elliptical part of the perturbed region.

We can give the following qualitative description of the phenomenon discovered. The significant pressure drop between the points K_1 and K_2 means that its equalizing downstream causes a sharp pressure drop behind the internal shock wave (Fig. 2b). At the same time, the wall streamlines which slope to the side of the edge of the wing because the point K_1 lags behind the position of the plane shock on the equivalent wedge acquire a negative curvature and increase the slope to the side of the edge. At the same time, the streamlines in the central part of the flow deviate even more from the chord of the wing under the influence of the positive pressure gradient. After equalizing the pressure in the interior part of the elliptical flow region, the wall streamlines, which have obtained additional transverse velocity (on the sphere) to the side of the edge of the wing, are retarded, acquiring a positive curvature, and this leads to an increase in the pressure along the wall of the wing (Fig. 2b), which causes a further deviation of the streamlines in the central part of the flow from the edge of the wing and forces back the streamlines in the neighborhood of the contact discontinuity to the side of the plane of symmetry. The ascent of the Ferri point is also a consequence of such a process. However, the streamlines running along the wall of the wing reach the edge of the wing and, under the influence of the negative pressure gradient, depart asymptotically in the plane of symmetry toward to the singular

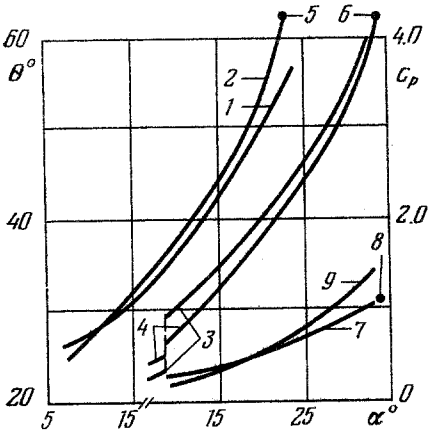

Fig. 3

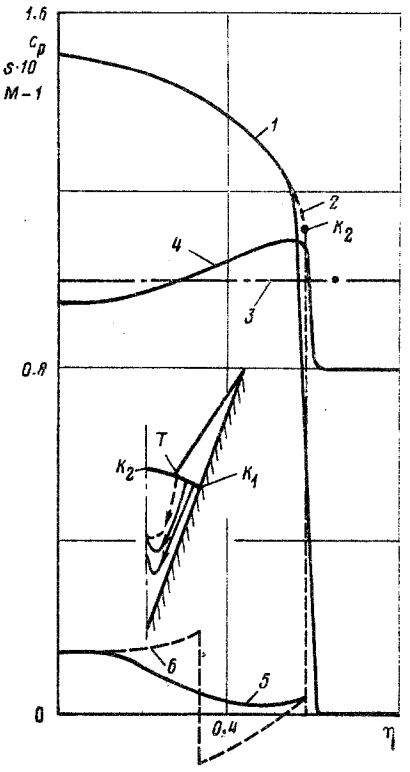

Fig. 4

ray (the Ferri point).

The flow scheme described will be realized for as small a deviation as required of the regime of flow past the wing from the standard regime ($\alpha \leq 33.8^\circ$), when the position of the bridge-shaped shock tends to the position of the plane shock wave lying in the plane of the leading edges of the wing (Fig. 3, curve 3), since in the wall flow region high-pressure stream jets are now present, directed to the side of the edge of the wing.

This step-by-step description of the process leading to the ascent of the Ferri point, based on the analysis of the boundary conditions for the system of shock waves bounding the elliptical flow region on the sphere, is qualitative. However, it can be confirmed that a necessary condition for the ascent of the Ferri point is the presence, in the wall flow region behind the internal shock of the Mach shock wave configuration, of gas particles moving to the side of the edge of the wing, with a higher total pressure on the sphere than the gas particles passing the bridge-shaped shock in the neighborhood of the plane of flow symmetry.

At the same time, as the pressure coefficient C_p behind the bridge-shaped shock K_2 (Figs. 2b, 3, curve 7) tends to its value on the equivalent wedge in the standard flow regime as $\alpha \to 33.8^\circ$ (Fig. 3, point 8), the maximum pressure coefficient in the perturbed region (Fig. 3, curve 9) increases monotonically and significantly exceeds its value behind the bow shock wave, this being associated with the retardation of the high-pressure wall stream jets passing the oblique—normal shock system.

The nature of the dependences of the position θ of the shocks on the wall of the wing with the apex angle $\beta = 45^\circ$ and in the plane of flow symmetry is the same as for the wing with the apex angle $\beta = 30^\circ$ (Fig. 3).

The intersection of curves 1 and 2 and the discontinuity in curves 3 and 4, corresponding to the standard flow regime of the inner wing with the edge 1 (point 1, Fig. 1b), occur for $\alpha = 24.8^\circ$.

The analysis of the results of the calculations showed that for $\alpha < 24.8^\circ$ the structure of the conical streamlines in the perturbed region does not differ from the standard when the Ferri singularity is at the break point of the transverse contour of the V-shaped wing. However, on the transition to the flow regimes with Mach interaction of the shock waves coming from the leading edges ($\alpha > 24.8^\circ$), the flow

structure in the perturbed region is rearranged at once, in contrast to what occurred in the flow past the wing with the angle $\beta = 30^\circ$.

At the triple points of the Mach configuration of shock waves for all angles of attack $\alpha > 24.8^\circ$ a shock polar interaction of the type shown in Fig. 2b is realized. The Mach numbers of the unperturbed flow velocity normal to the conical rays going through the point T are $M_n \geqslant 2.25$. Thus, in these cases, particles with a total velocity direction toward the edge of the wing, and with a greater total pressure on the sphere than the particles passing the bridge-shaped shock in the neighborhood of the plane of symmetry are present in the wall region behind the internal shock. Therefore, for $\alpha > 24.8^\circ$, the Ferri point will ascend and be located inside the elliptical region of the conical flow.

Figure 4 gives the distributions of the parameters in the plane of flow symmetry near the wing with the angle $\beta = 45^\circ$ for the angle of attack $\alpha = 32.5^\circ$. A qualitative flow scheme in the perturbed region is shown in the same place (Fig. 4, the notation of the curves is the same as in Fig. 2). We note that for $\alpha = 32.5^\circ$ the attached shock on the equivalent wedge placed in the uniform flow behind the shock wave on the leading edge no longer exists and, hence, it would be wrong to attempt to determine whether or not there exists near the wing a flow with a shock attached to the leading edges for the given angle of attack from the existence of a shock wave on the equivalent wedge.

As has already been noted above, in the flow past the wing with the apex angle $\beta = 90^\circ$ on the inner wing with the edge 1 (point 1, Fig. 1c) the standard flow regime is not realized, just as near the wing with $\beta = 45^\circ$. The standard regime exists only on the inner V-shaped wing with the leading edge 2 (point 2, Fig. 1c) for the angle of attack $\alpha = 20.5^\circ$. For the angles of attack $\alpha > 20.5^\circ$ near the inner wing with the leading edge 1 a Mach configuration of the shock waves is realized with the same qualitative characteristics as for the wing with the angle $\beta = 45^\circ$ for $\alpha > 24.8^\circ$. However, in this case, the wing wall is the plane of flow symmetry for the inner wing and a flow scheme with two Ferri points on the walls of the initial wing is realized in the interior flow region for $\alpha > 20.5^\circ$. Figure 5 gives the flow scheme for the angle of attack $\alpha = 27.5^\circ$ as an example.

We turn to the question of the existence of conical flow near V-shaped wings of finite length. It is natural to assume that, when regions with total velocity less than the critical velocity arise in the perturbed flow, the perturbations leaving the the trailing edge of the wing will penetrate upward through the subsonic part of the flow and, therefore, conical flow near the wing will not be realized.

For wings with apex angles $\beta = 30$ and 45°, the critical velocity behind the shock on the equivalent wedge placed in a uniform flow near the wall of the wing is reached for lower angles of attack than those up to which the calculation was made. This was found possible because of the lag of the position of the internal shock behind the position of the shock wave on the equivalent wedge. Thus, for the wing with the angle $\beta = 45^\circ$, it is possible to make the calculation up to the angle of attack $\alpha = 32.5^\circ$. The attempt to obtain a solution of the problem for the angle of attack $\alpha = 32.75^\circ$ did not give the desired result. The solution did not become steady. At the same time, neither the external nor the bridge-shaped shock have yet reached the positions for which the flow behind them have the velocity of sound. This indicates that the critical velocity in the flow arises not behind the shocks, but inside the elliptical region of the conical flow.

The number $M = 1$ will first be reached on the streamlines in the plane of symmetry, since the bridge-shaped shock has its maximum intensity here and the pressure behind it increases toward the edge of the wing. Thus, the qualitative rearrangement of the flow structure, associated with the ascent of the Ferri point, is the reason why the critical velocity arises earlier in the interior flow region than behind the bridge-shaped shock.

Figure 4 gives the curve 5 of the distribution of the total velocity Mach number in the plane of flow symmetry, calculated using the parameter field obtained in the numerical solution. The curve indicated has a minumum behind the shock, downstream. The minimum total velocity Mach numbers M are shown in Fig. 6 as functions of the angle of attack α (curves 1, 2, $\beta = 45, 90^\circ$). Their extrapolation (the broken curves)

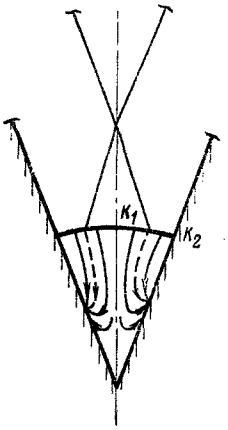

Fig. 5

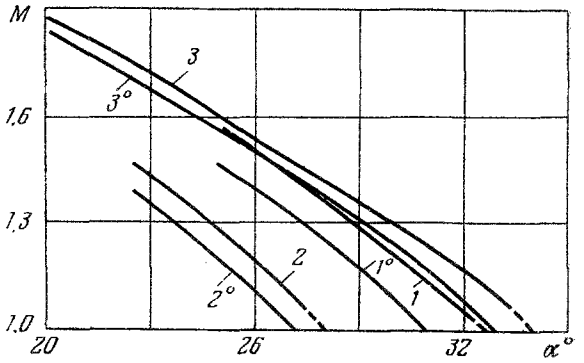

Fig. 6

to large angles of attack shows that the critical velocity in the numerical solution must be reached for the wing with the angle $\beta = 45^\circ$ for the angle of attack $\alpha \approx 32.75^\circ$, and for the wing with the angle $\beta = 90^\circ$ for $\alpha \approx 27.8^\circ$, for which the calculation did not stabilize.

It should be noted, however, that curve 5 in Fig. 4 describes the variation of the total velocity Mach number extremely approximately, since the Ferri singularity in the numerical solution is smeared and, hence, there is an inaccurate representation of the components of the total velocity in its neighborhood. The distribution of the Mach number can be made more precise using its values behind the shock wave and in the neighborhood of the edge of the wing, and the pressure distribution as the most conservative parameter in the numerical calculations. Assuming that the position of the Ferri point is the same as the position of the maximum gradient of the entropy function (curves 4 in Figs. 2b and 4), the increase and decrease of the Mach number for the streamlines running from the edge of the wing and from the shock toward the Ferri point can be calculated, respectively, in accordance with the isentropic flow equations. The results of such calculations are plotted by the broken curves 6 in Fig. 4. The Mach number on the axis of symmetry at the Ferri point undergoes a discontinuity, this being associated with the different boundary conditions for the streamlines entering into the Ferri point.

The dependence of the minimum M numbers at the Ferri point, found in accordance with the isentropic equations, on the angle of attack α is shown in Fig. 6 by the curves 1° and 2°, respectively, for the wings with the angles $\beta = 45$ and 90°. Hence, it follows that the critical value of the total velocity will, in fact, be reached for $\beta = 45$ and 90°, respectively, for $\alpha = 31$ and 27° and the conical flow near the V-shaped wings of finite length for the indicated values of the angle β for large angles of attack will not exist.

The dependences of the minimum total velocity Mach numbers in the interior flow region near the wing with the apex angle $\beta = 30^\circ$, obtained in the numerical solution and in accordance with the isentropic equations, are shown by curves 3 and 3° in Fig. 6. Consistent with the given calculations in accordance with the isentropic equations (curve 3°), the conical flow will not exist near the wing of finite length with the angle $\beta = 30^\circ$ for angles of attack less than the calculated angle ($\alpha = 33.8^\circ$).

Thus, the ascent of the Ferri point leads to the fact that the conical flow ceases to exist for angles of attack less than the calculated angle, but for $\alpha \geqslant 33.8^\circ$, it again becomes conical, while for $\alpha > 33.8^\circ$ it is with the detached shock wave on the leading edges [7].

LITERATURE CITED

1. V. V. Rusanov, "Calculation of the interaction of unsteady shock waves with obstructions," Zh. Vychisl. Mat. Mat. Fiz., 1, 271 (1961).
2. V. I. Lapygin, "Calculation of supersonic flow past V-shaped wings by the method of stabilization," Izv. Akad. Nauk SSSR, Mekh. Zhidk. Gaza, No. 3, 180 (1971).

3. A. L. Gonor, N. A. Ostapenko, and V. I, Lapygin, "The conical wing in hypersonic flow," Lect. Notes Phys., 8, 320 (1971).
4. V. I. Lapygin and N. A. Ostapenko, "Flow of supersonic gas past the windward side of a conical wing," Izv. Akad. Nauk SSSR, Mekh. Zhidk. Gaza, No. 1, 112 (1973).
5. V. I. Lapygin, "Solution of the problem of flow past a V-shaped wing with a strong shock on the leading edge," Izv. Akad. Nauk SSSR, Mekh. Zhidk. Gaza, No. 3, 114 (1973).
6. M. A. Zubin, V. I. Lapygin, and N. A. Ostapenko, "Theoretical and experimental investigation of the structure of supersonic flow past star-shaped bodies and their aerodynamic characteristics," Izv. Akad. Nauk SSSR, Mekh. Zhidk. Gaza, No. 3, 34 (1982).
7. M. A. Zubin and N. A. Ostapenko, "Experimental investigation of some features of supersonic flow past V-shaped wings," Izv. Akad. Nauk SSSR, Mekh. Zhidk. Gaza, No. 4, 130 (1975).
8. V. S. Gorislavskii, "Flow in a solid angle with large entropy differences," Uch. Zap. TsAGI, 13, 129 (1982).
9. G. N. Abramovich, Applied Gas Dynamics [in Russian], Nauka, Moscow (1976).

SOUND PROPAGATION IN A PLANE WAVE GUIDE WITH AN ELASTIC WALL SECTION

V. M. Aleksandrov and S. I. Boev

UDC 533.6.013.42

Problems of acoustic wave propagation in a plane wave guide whose walls are assumed to be undeformed with the exception of a section of finite length whose bending is described by the thin plate theory equations in the framework of the Kirchhoff—Love hypotheses are considered. The soundproofing characteristics of the wave guide described and the stability of the forced oscillations of the system considered are investigated. Formulations of the problem of active vibroacoustic protection and the problem for the peristaltic pump are given. Soundproofing in wave guides has been considered in a number of papers, a fairly complete review of which is given in [1].

1. We consider the problem of generating acoustic waves in a plane wave guide (Fig. 1) by means of the time-periodic load $q(x, t) = Qe^{-i(\eta x+\omega t)}$ applied to the elastic section of the wall. The equations of the Kirchhoff—Love thin plate theory are used to describe the deformation of the elastic element of the wave guide wall. It is assumed that the wave guide is filled by a perfect compressible fluid, in which the wave processes will be described by the acoustic approximation equations.

Eliminating the time variable and assuming that the time dependence of all the unknown quantities is expressed by the factor $e^{-i\omega t}$ in the coordinate system shown in Fig. 1, we obtain the following set of equations:

$$\Delta\varphi+\frac{\omega^2}{c^2}\varphi=0, \quad x\in(-\infty,+\infty), \quad y\in(0,H) \tag{1.1}$$

$$y=0: \ \frac{\partial\varphi}{\partial y}=0, \quad x\in(-\infty,+\infty), \quad y=H: \ \frac{\partial\varphi}{\partial y}=0, \quad |x|>a \tag{1.2}$$

$$\frac{\partial\varphi}{\partial y}=-i\omega w, \quad Dw^{IV}-\rho\omega^2hw=i\rho_0\omega\varphi-Qe^{-i\eta x}, \quad |x|<a, \ w(\pm a)=w'(\pm a)=0 \tag{1.3}$$

Here φ is the acoustic potential, ρ_0, c are, respectively, the density of the fluid and the velocity of sound in it, w is the vibrational mode of the plate, D, h are the cylindrical rigidity and the thickness of the plate, ρ is the material density of the plate, H is the distance between the rigid walls of the wave guide, and *a* is the half-length of the elastic insertion. We note that Eqs. (1.3) describe the conditions

Moscow, Rostov-on-Don. Translated from Izvestiya Akademii Nauk SSSR, Mekhanika Zhidkosti i Gaza, No. 1, pp. 132-139, January-February, 1986. Original article submitted February 8, 1985.

 0015-4628/86/2101-0112$12.50